Poleward shift of Circumpolar Deep Water threatens East Antarctic Ice Sheet

Authors: Laura Herraiz-Borreguero*[1] and Alberto C. Naveira Garabato[2]
*Corresponding author: Laura.HerraizBorreguero@csiro.au

[1]Commonwealth Scientific and Industrial Research Organization Oceans and Atmosphere, and Centre for Southern Hemisphere Oceans Research, Hobart Tasmania, Australia

[2] Ocean and Earth Science, University of Southampton, Southampton, UK

Abstract

Future sea-level rise (SLR) projections carry large uncertainties, mainly driven by the unknown response of the Antarctic Ice Sheet to climate change. During the past four decades, the contribution of the East Antarctic Ice Sheet to SLR has increased. However, unlike for West Antarctica, the causes of East Antarctic ice-mass loss remain largely unexplored. Here, using oceanographic observations off East Antarctica (80º-160ºE) we show that mid-depth Circumpolar Deep Water has warmed by 0.8-2.0°C along the continental slope between 1930-1990 and 2010-2018. Our results indicate that this warming may be implicated in East Antarctic ice-mass loss and coastal water-mass reorganisation. Further, it is associated with an interdecadal, summer-focused poleward shift of the westerlies over the Southern Ocean. As this shift is predicted to persist into the 21st century, the oceanic heat supply to East Antarctica may continue to intensify, threatening the ice sheet's future stability.

Main text

The Antarctic Ice Sheet has been losing mass at an accelerated rate since the 1970s[1], and now accounts for ~15% of global SLR[5]. In West Antarctica, the ice-mass loss has been attributed to a wind-driven increase in the transfer of warm CDW toward the floating ice shelves[2,3]. As the ice shelves melt, their mechanical buttressing of tributary glaciers is reduced, leading to

faster glacier flow toward the coast and greater freshwater input to the ocean[6]. Consistent with this view, observed interdecadal trends in West Antarctic ice-mass loss have been linked to warming of the continental shelf's deeper oceanic layers, with either the evolving decadal-mean temperature[7] or amplitude of interannual temperature variability[2,8] posited to exert the key melting-controlling role. A singular feature of West Antarctic change is that the measured ocean warming occurs on the continental shelf[2], rather than in the Antarctic Circumpolar Current (ACC) offshore[2], pointing to a perturbed rate of CDW transport across the shelf break as the warming's underpinning factor.

The ice-mass loss in East Antarctica is dominated by changes in the Wilkes Basin[9] (100º-142ºE), in the eastern Indian Ocean sector. Its causes remain both undetermined and little probed. The presence of modified CDW in proximity to several ice shelves[10,11,12] hints at an increased delivery of heat from the ACC plausibly being implicated in regional ice-mass loss. However, evidence of such an increase, and knowledge of its possible forcings, are currently scarce. While investigations of the interdecadal evolution of CDW temperature reveal a widespread, persistent warming to the north of and within the ACC, equatorward of ~60ºS[7,13,14], there has been little indication of robust long-term temperature changes further to the south. Only recently, two studies[15,16] have put forward the suggestion that a CDW warming might be underway poleward of ~60ºS, possibly linked to a southward shift of the ACC's southern boundary in the eastern Indian region (115-150ºE)[15] or a CDW shoaling south of Tasmania[16]. However, spatio-temporal sampling limitations prevented these works from assessing the generality of CDW warming across the Indian Ocean sector of East Antarctica and, crucially, whether such warming (i) extends all the way to the continental slope, the access point of CDW to the East Antarctic shelves, and (ii) reaches the East Antarctic Ice Sheet. Performing this assessment is the goal of our paper.

Deep warming off East Antarctica

In this work, we determine the interdecadal evolution of CDW properties off the Indian Ocean sector of East Antarctica (80º-160ºE) between 1930 and 2018 from oceanographic observations (see Suppl. Mat.), and investigate the drivers and possible ice-sheet impacts of the observed CDW changes. Our focus on the Indian Ocean sector stems from this region's glaciers contributing the bulk of East Antarctic ice-mass loss in recent decades[9,17,18]. Our evaluation of long-term water-mass variability off East Antarctica presents two important advances relative to previous studies[15,16], in that our dataset: (i) has a substantially improved spatial coverage of the seasonally ice-covered areas near the East Antarctic margins, particularly over the continental slope and shelves; and (ii) spans a longer (by several decades) period.

We commence by examining potential temperature (θ) changes at 400 m along the East Antarctic continental slope (here bounded by the 700 m and 3000 m isobaths; Figure 1) and in the open ocean to the north (Figure 2a). This vertical level is chosen because it is close to the upper part of the CDW intruding onto the continental shelves off the Indian East Antarctic sector, in areas where the shelf break is deeper than 400-500 m[19]. Similar temperature changes can be observed as deep as 700-900 m, and throughout the density layers between 27.95 and 28.15 kg m^{-3} containing CDW. The measurements reveal that a generalized warming of up to 0.5ºC between prior to the 1990s and the 2010s has occurred in the open ocean off East Antarctica (Fig. 2a). This temperature change is broadly in line with those estimated previously in the same region[7,15,16] and, remarkably, it is concurrent to an even more pronounced warming of 0.8-2ºC (or 0.1-0.4ºC per decade) over the continental slope (Fig. 1). The warming signals are qualitatively insensitive to the choice of multidecadal interval, being present irrespective of whether the relatively data-poor pre-1990s period is included in the analysis. The

continental slope warming is strongest near ice shelves that are thinning[20] and/or have retreating grounding lines[1,18], such as the Denman (~100ºE) and the Vanderford (~110ºE) glaciers (Figs. 1c-d and 2a). Since the CDW over the continental slope sources the heat transferred toward the ice shelves across the Antarctic Slope Front[21], which is topographically-pinned to the shelf break[22], a warming of such source CDW might expectedly drive the observed ice mass loss.

The CDW warming off East Antarctica could have either or both of two possible causes: a warming of the CDW within the ACC and its southern environs[13], associated with e.g., an enhanced cross-ACC isopycnal transfer of CDW[15]; or a poleward expansion of the ACC's hydrographic structure, which entails an equatorward increase in the climatological temperature of CDW of 0.2-1°C/100 km[23,24] (Fig. S1). To quantify the importance of each of these factors in CDW warming (see Methods), we re-map the distribution of θ at 400 m onto dynamic height for the period before 1990 and for 2010-2018; we compute the θ change in that coordinate system between the two periods (Fig. 2a); and we calculate the percentage of the θ change in geographical space that is associated with a change in dynamic height (Fig. 2b). This shows that the bulk (typically >60%) of the measured CDW warming has occurred in association with a dynamic-height increase (by ~0.2 m^2 s^{-2}), which corresponds to a southward migration of dynamic-height contours by 1°-2° of latitude (Fig. S2). This suggests that the CDW warming is primarily underpinned by a poleward encroachment of the ACC's southern flank onto the Indian Ocean East Antarctic continental slope, in line with recent observational and modelling diagnostics of hydrographic variability in the eastern open-ocean sector of our study region[15,16].

To substantiate this result, we examine the variability in the position of the ACC's southern flank (S-ACC) from two independent data sources. On one hand, the S-ACC is defined as the location at which the 1.8°C isotherm embedded within CDW outcrops into the remnant winter mixed layer[24] (Fig. S3), a measure of the poleward reach of the CDW's warm core that straddles traditional definitions of hydrographic fronts in the southern ACC (see Suppl. Mat.). On the other hand, the S-ACC consistently corresponds with a sea-surface height (Ψ_{SSH}) value of -1.18 m (Methods), such that it can be tracked from satellite altimetric observations. The evolution of both estimates of the S-ACC position between the 1990s and 2010s is found to be coherent, with a southward shift of typically 100-200 km over that period (Figs. 1e and S2). While the S-ACC never quite reaches the Indian Ocean East Antarctic continental slope, the dynamic-height increase associated with the S-ACC's poleward translation extends through to the slope, where dynamic height has risen at ~0.005 $m^2\ s^{-2}$ per decade over much of the Indian Ocean sector (Figs. S2 and S4). Thus, we surmise that the ACC's southward expansion off East Antarctica in recent decades may plausibly explain the CDW warming at the continental slope. Within this explanation, the stronger CDW warming in this area (Figs. 1, 2a) is an expected result of the locally-enhanced meridional temperature gradient[22] (Fig. S1), although a substantial contribution from other, shelf break-focused processes[12,21] (due to e.g., a change in local wind forcing) analogous to those prevalent off West Antarctica[2,8] may also be at play. Our rationalisation of the observed CDW warming as arising from a poleward migration of the S-ACC's hydrographic structure is further endorsed by an analysis of changes in θ along density surfaces (see Supp. Mat., and Figs. S5 and S6), which yields patterns of CDW warming compatible with such interpretation: a southward translation of the meridional θ gradient characteristic of the S-ACC region would result in a widespread warming, the magnitude of which would peak near the continental slope (where the meridional θ gradient is largest) and decay to zero toward the north (where the meridional θ gradient approaches zero; see Fig. S6).

Probable causes of CDW warming

A window into the likely causes of the southward translation and warming of CDW off East Antarctica is provided by the climatological relationship between the region's atmospheric configuration and oceanic circulation. This relationship is examined here using austral summertime (December-February) atmospheric data for three reasons. First, this is the only season for which multiple atmospheric reanalyses exhibit consistent tendencies in the properties of the major wind jets over the last four decades, with other seasons subject to greater inter-reanalysis uncertainties[25]. Second, it is in summer that: the Antarctic Slope Front is weakest[26], following the annual minimum in the intensity of easterly winds over the continental slope[27]; and CDW is shallowest at the slope (Fig. S7), thereby exerting the most influence on the continental shelf[26]. And finally, a sustained altimetric estimate of the S-ACC's location is enabled by minimal sea ice extent only in summer.

The Southern Ocean's Indian sector is forced by dominant westerly winds to the north of 63°-66°S and by easterly winds to the south of that latitude[27], implying a prevalence of negative wind stress curl (WSC) across the region (Fig. 3b). This wind forcing arrangement generates a surface Ekman flow divergence (leading to a minimum in Ψ_{SSH}) around the westerlies-easterlies transition, which is associated with a relative maximum in climatological WSC (Fig. 3b); and convergences of that flow (leading to maxima in Ψ_{SSH}) at the Antarctic coast and within the ACC to the north of ~50°S. The surface geostrophic ocean circulation exhibits a reversal from eastward flow around the S-ACC, to westward flow at the continental slope[15,21,24,28]. The westward-to-eastward flow reversal is approximately aligned with the westerlies-easterlies transition (Fig. 3b, solid black and red lines), such that the S-ACC's

latitude – and thus the poleward reach of the CDW's warm core (Fig. S1) – is expected to be strongly influenced by that transition via barotropic dynamics[29].

Assessment of the interannual evolution of the westerlies-easterlies transition over the last four decades endorses this expectation. Substantial meridional shifts of up to several hundred kilometres occurred in the transition's location, manifested in year-to-year WSC fluctuations of up to ~5 × 10^{-8} N m^{-3} (Fig. 3a). An interdecadal trend in the WSC anomaly of -1.81× 10^{-10} N m^{-3} per decade, $p<0.01$) (Fig. 3a) signals a southward migration of the ACC's negative WSC zone and, thereby, of the westerlies-easterlies transition, of up to ~200 km between the 1990s and 2010s (cf. blue and red solid lines in Fig. 2). This pattern of change was broadly paralleled by the meridional displacement of the S-ACC (blue and red dashed lines in Fig. 3b), suggesting that the poleward shift of the westerlies underpinned the observed southward expansion of CDW in the open ocean off East Antarctica (Fig. 2) and the associated CDW warming over the continental slope (Fig. 1). The physical robustness of such control is compatible with a recent modelling study[15], which reproduced the S-ACC's poleward displacement and open-ocean CDW warming documented here in simulations forced with realistic winds.

The reorganization of the winds off East Antarctica responsible for the observed CDW changes was associated with the evolving state of the Southern Annular Mode (SAM) – the leading mode of atmospheric variability across the extratropical Southern Hemisphere[30]. This association is elicited by the significant correlation between the WSC anomaly and the SAM index (Fig. 3a), which may be understood as follows. An anomalously positive SAM state is systematically manifested in an intensification and contraction of the polar vortex. This results in a strengthening and southward translation of the westerlies[4] and a weakening[27] and poleward shift of the easterlies (Fig. 3b), leading to an increasingly negative WSC around the S-ACC.

The reverse scenario occurs for an anomalously negative SAM state. These well-established interannual relationships (Fig. 3a) suggest that the SAM's summer-focussed positive interdecadal trend since the 1960s, which has been attributed to anthropogenic forcing[31], may account for the meridional migration of the westerlies-easterlies transition identified in our work. As the easterlies exert an important role in controlling the depth of CDW over the continental slope, it is likely that the SAM-associated, interdecadal weakening of the summertime easterlies[27] may have contributed to the locally-magnified warming of CDW at the slope (Fig. 2a) and, through shoaling, enhanced the CDW's on-shelf access[32].

Impact on the East Antarctic margins

We have suggested that a CDW warming, induced by a SAM-related, wind-forced poleward displacement of the S-ACC and amplified at the continental slope, may have contributed to the East Antarctic ice-mass loss[9] and extensive grounding line retreat[18] in recent decades. This proposition relies on the existence of a physical link between the S-ACC's proximity to East Antarctica and the rate of regional ice-mass loss. To elucidate this link, we put forward two lines of evidence. First, we document a water mass shift that may have occurred between the summers of 1997 and 2012 at Vincennes Bay (~108ºE), where continental shelf waters have direct ice-shelf cavity access within our study domain (Fig. 4). Here, warm (of up to 0.5°C) modified CDW most recently flooded a continental shelf area[33] that was filled with considerably colder (near-freezing) coastal polynya-produced Dense Shelf Water (DSW) in 1997. This apparent water mass shift occurred despite the stability in polynya-driven sea ice production, and polynya area, between 1992 and 2012[ref[34]]. As polynya-driven sea ice production forces DSW formation[35], a decline in DSW concurrent to unchanging sea ice production is consistent with a greater on-shelf transfer of warm CDW and, predictably, enhanced ice shelf melting – which was indeed manifest in the fast grounding line retreat of

the Vanderford glacier[1] (17 km between 1996 and 2016). These changes are as would be expected if an intensification in the CDW-mediated heat supply from the S-ACC drove increased regional ice-mass loss.

Second, we cross-examine the interannual variability in the altimetry-based latitude of the S-ACC and thickness of major East Antarctic ice shelves[20] over their concurrent (1994-2012) period (Fig. S8). Despite several non-trivial caveats in the estimation and interpretation of the thickness data (see Suppl. Mat.), the latitude of the S-ACC to the north of each major ice shelf (e.g., West, Shackleton and Dibble) is found to exhibit a significant multi-annual linear trend of the same sign as the trend of that ice shelf's thickness. This result is compatible with the S-ACC's proposed role in delivering warm CDW against the continental slope (Fig. 2a), whence CDW may flood the continental shelf (Fig. 4). Additional support for this role is provided by the close spatial correspondence of the warmer CDW (warmer than -0.5ºC) with the glaciers whose ice shelves have thinned[17] and grounding lines retreated[9] most rapidly (Fig. S8), namely: West, Denman[36], Vanderford[33], Totten[10] and Dibble[19]. East of 145°E, data scarcity precludes us from confidently exploring the influence of CDW on the melting of Cook and Rennick ice shelves.

Conclusions and Outlook

The increased loss of mass from the Antarctic Ice Sheet in recent decades has comparably affected both of the ice sheet's major sectors (West and East Antarctica), fuelled almost certainly by enhanced oceanic heat delivery to the ice shelves[2,8,10]. In West Antarctica, such intensified delivery is thought to have been driven by localized wind-forcing perturbations along the continental slope facilitating the on-shelf transfer of warm CDW[2], with changes in offshore CDW properties playing a modest role. The key perturbations in the along-shelf break

winds are tightly coupled to the Amundsen Sea Low[3], whose state is modulated by tropical Pacific climate variability (including the El Niño-Southern Oscillation)[37]. Accordingly, tropical Pacific climate is projected to strongly steer the West Antarctic Ice Sheet's evolution over the remainder of this century[8].

In this work, we have unravelled several threads of evidence which, despite substantial individual caveats, coalesce into a coherent picture of East Antarctic change that may be distinct from that in West Antarctica. Thus, in the Indian Ocean sector of East Antarctica, the enhanced oceanic heat transport responsible for the growing ice mass loss[1] has likely been underpinned, at least in part, by CDW warming at the continental slope. Such warming resulted from the S-ACC's southward migration, which was associated with a summer-focussed, large-scale poleward translation of the mid-latitude westerlies. As this shift of the westerlies is coherent with a positive tendency of the SAM[32], our results indicate that this climatic mode is likely to exert a major influence on the East Antarctic Ice Sheet's future evolution.

This inference carries important implications. A consistent prediction of 21st-century climate projections[37,39] is that the SAM's recent summertime positive trend (and its attendant southward displacement of the westerlies) will continue for coming decades under all plausible greenhouse-gas emission scenarios, driven by radiative forcing linked to increasing greenhouse-gas levels[31,38]. If this prediction comes to be, we may expect that the S-ACC's poleward translation and CDW warming off East Antarctica documented here will proceed unrelentingly into the future and, ultimately, may compromise the ice sheet's stability in this sector. The unfolding of such a scenario could arguably be hastened by positive ice sheet-ocean feedbacks. Specifically, as increased ice-mass loss freshens and stratifies the upper ocean, the stronger stratification is envisaged to lessen the capacity of coastal polynyas to

trigger DSW production on the continental shelf via full-depth convection, thereby enabling a greater penetration of warm CDW toward the ice shelves and further enhancing ice-shelf melting[33,39,40]. The collection of evidence presented in this work – in particular, the apparent hydrographic transition observed in the Vincennes Bay region (Fig. 4) – suggests that these feedbacks may already be underway.

Acknowledgements

We gratefully acknowledge grant support for the authors as follows: LHB from the European Research Council Horizon 2020 Marie Skłodowska-Curie Individual Fellowship, through grant number 661015, and the Centre for Southern Hemisphere Oceans Research (CSHOR, Hobart, Australia); ACNG from the Royal Society and the Wolfson Foundation. For the purpose of open access, the author has applied a Creative Commons Attribution (CC BY) licence to any Author Accepted Manuscript version arising

Author contributions Statement

LHB proposed the research, led data analysis and prepared the figures. LHB and ANG interpreted the results and wrote the manuscript.

Competing interests Statement

We declare no competing interests.

Figure Captions

Figure 1. Warming of the Indian Ocean sector of the East Antarctic continental slope. (a-d) and (f-g), Temporal evolution of potential temperature at 400 m over the East Antarctic

continental slope,computed in geographical space. The solid blue (green) line shows a linear regression fit for all the data available (for the data available since 1990), and the dashed blue (green) lines provide 95% confidence intervals. (*) denotes that the regression model is not significant to the 95% confidence according to our bootstrap analysis (e) Spatio-temporal distribution of the hydrographic observations (dots, coloured by year) considered in the other panels. The vertical lines indicate the latitude at which the 1.8ºC isotherm outcrops before 2000 (blue) and in 2010-2018 (red). The contours show the average location of the summer (January-March) $\boldsymbol{\Psi}_{SSH}$ = -1.18 m contour, indicative of the S-ACC, in 1992-2000 (blue) and in 2010-2018 (red). The red dashed line marks the extension of this $\boldsymbol{\Psi}_{SSH}$ contour to the south of the Kerguelen Plateau. The 400 m, 1000 m, 2000 m and 3000 m isobaths are shown as thin grey contours. Ice shelf thickness change rates[20] (m/decade) are shown for the West, Shackleton-Denman, Totten and Dibble ice shelves.

Figure 2. **Changes in CDW potential temperature and their link to the southward migration of the S-ACC**. (a) Potential temperature change at 400 m between 1930-1989 and 2010-2018, computed in geographical space. (b) Percentage of the potential temperature change at 400 m that is explained by a change in dynamic height. Positive (negative) values show the areas in which frontal displacements effect a same-signed (an oppositely-signed) potential temperature change to that observed. The lines indicate the 1992-2000 (blue) and 2010-2018 (red) summer-average latitude of the $\boldsymbol{\Psi}_{SSH}$ = -1.18 m contour, which denotes the position of the S-ACC. The 400 m, 1000 m, 2000 m and 3000 m isobaths are shown as thin grey contours. Areas outside our study region have been masked.

Figure 3. **Changes in wind stress curl and their link to the southward migration of the S-ACC.** (a) Summer (December-February) wind stress curl anomaly relative to the time mean

over the 1979-2018 period over 59-62ºS / 80-150ºE (blue) (see Fig. S12). The blue thin line is the linear regression fit (which has a slope of -1.81×10^{-10} N m^{-3} per decade, $p<0.01$), bounded by 95%-confidence bounds (blue dashed lines). The red line is the Marshall SAM summer (December-February) index, and the thin red line shows the positive trend (p-value ~0.03, bounded by the 95% confidence bounds) in that index; (b) 1979-2018 mean summer (December-February) wind stress curl (N m^{-3}) in the eastern Indian Ocean sector of the Southern Ocean. The black and red contours indicate the location at which the meridional wind stress curl is zero in 1980-1985 and 2010-2015, respectively. The 400, 1000, 2000 and 3000 m isobaths are shown as grey lines.

Figure 4. Warming of Vincennes Bay. (a) Map of the Vanderford ice shelf in Vincennes Bay, showing the location of potential temperature and salinity profiles in 1997 (triangles) and 2012 (dots). The colour of the symbols is indicative of the maximum available heat (potential temperature (θ) minus the surface freezing temperature (θ_f)) to melt ice below 400 m. Coloured boxes delimit the region east (purple) and west (green) of the Vanderford ice shelf calving front. (b) Potential temperature and salinity vertical profiles. To aid clarity, the seal profiles found in the western flank of the ice shelf are shown in green, while the seal data in the eastern flank are shown in purple. The 1997 data is shown in blue. (c) Potential temperature-salinity diagram. The dashed black line denotes the surface freezing temperature. Water masses found below 400 m are highlighted: DSW: Dense Shelf Water; mCDW: modified Circumpolar Deep Water; and ISW: Ice Shelf Water. The black box shows where DSW is found in the diagram.

Figures

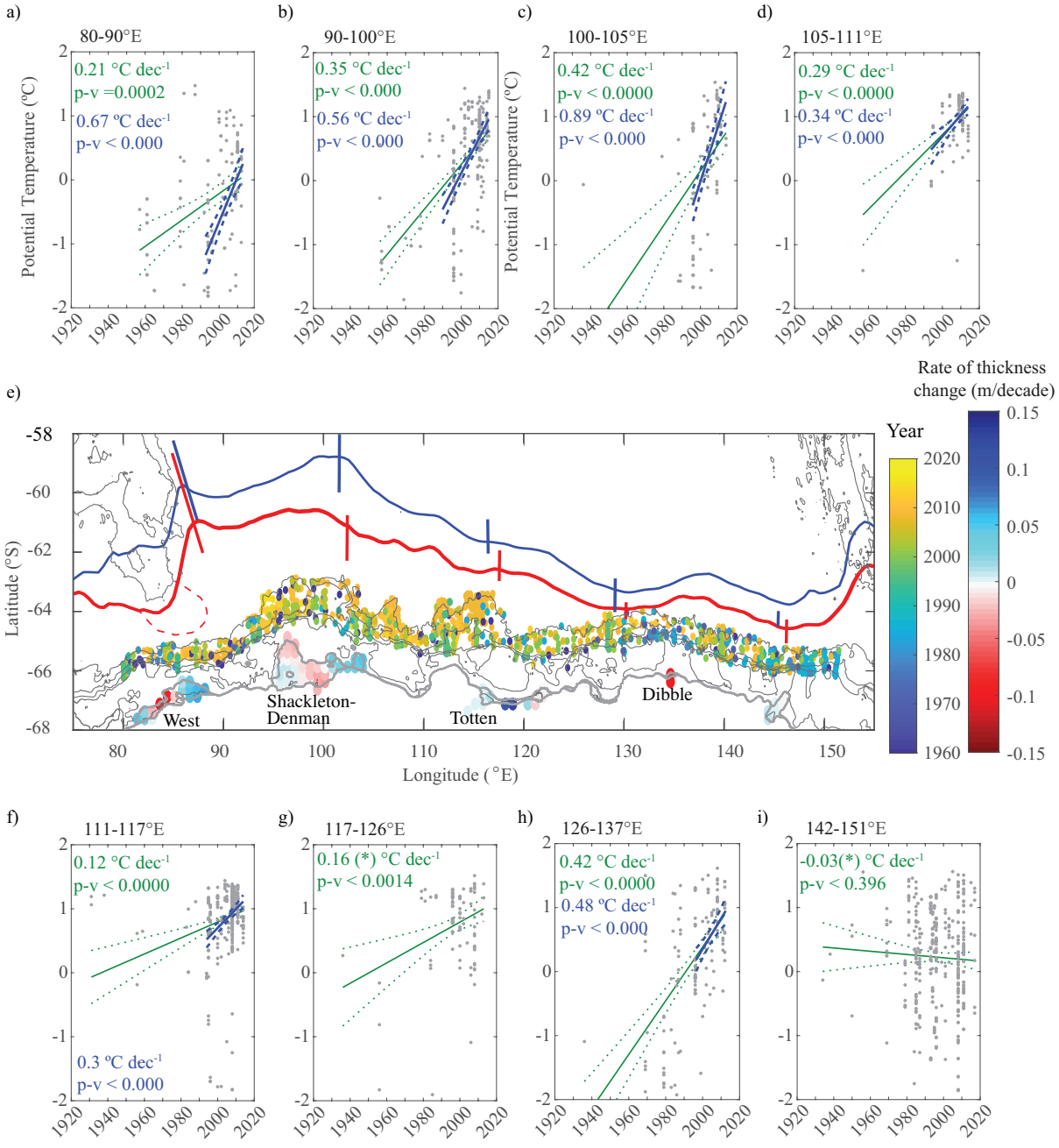

Figure 1. Warming of the Indian Ocean sector of the East Antarctic continental slope.

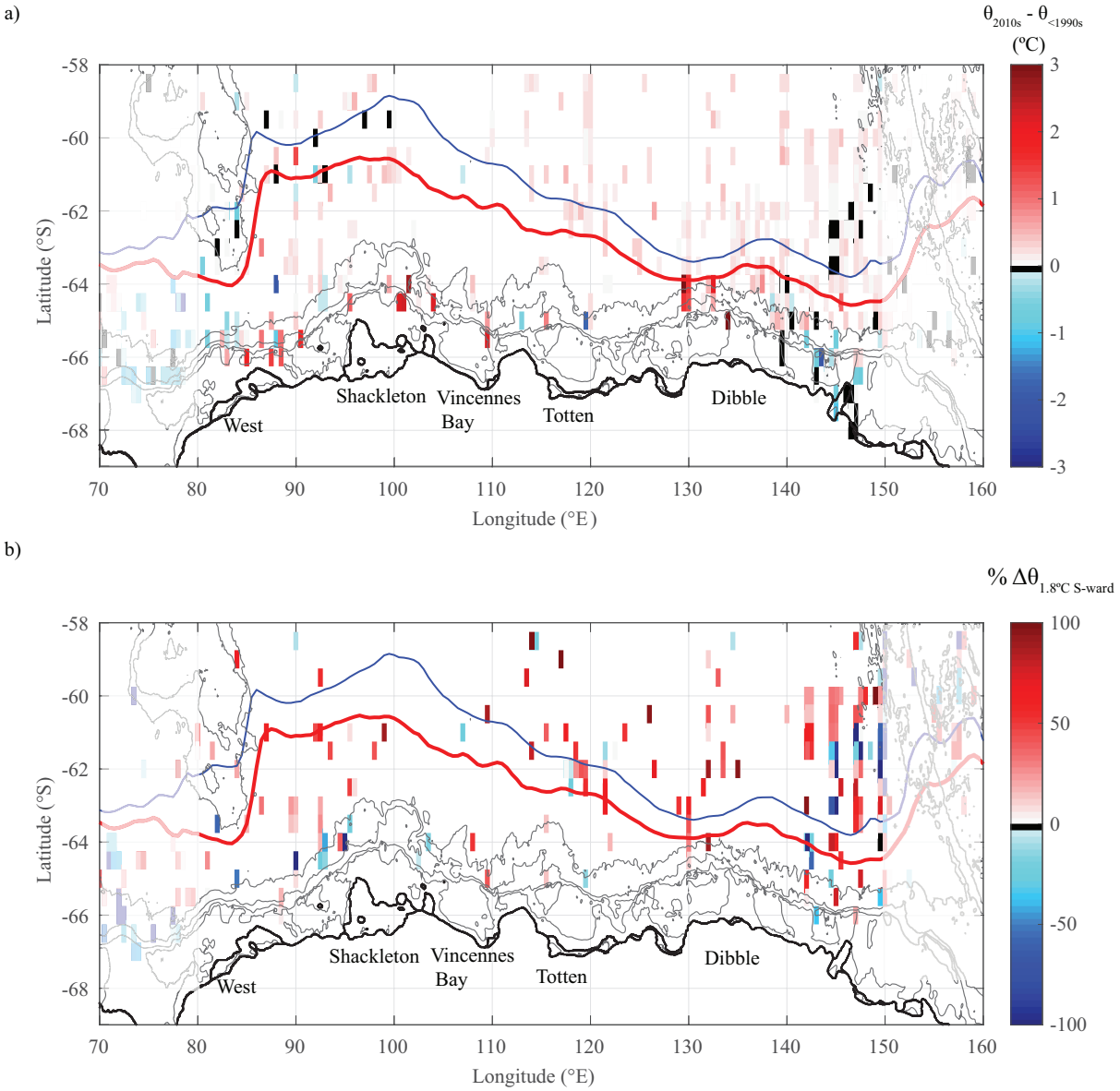

Figure 2. Changes in CDW potential temperature and their link to the southward migration of the S-ACC.

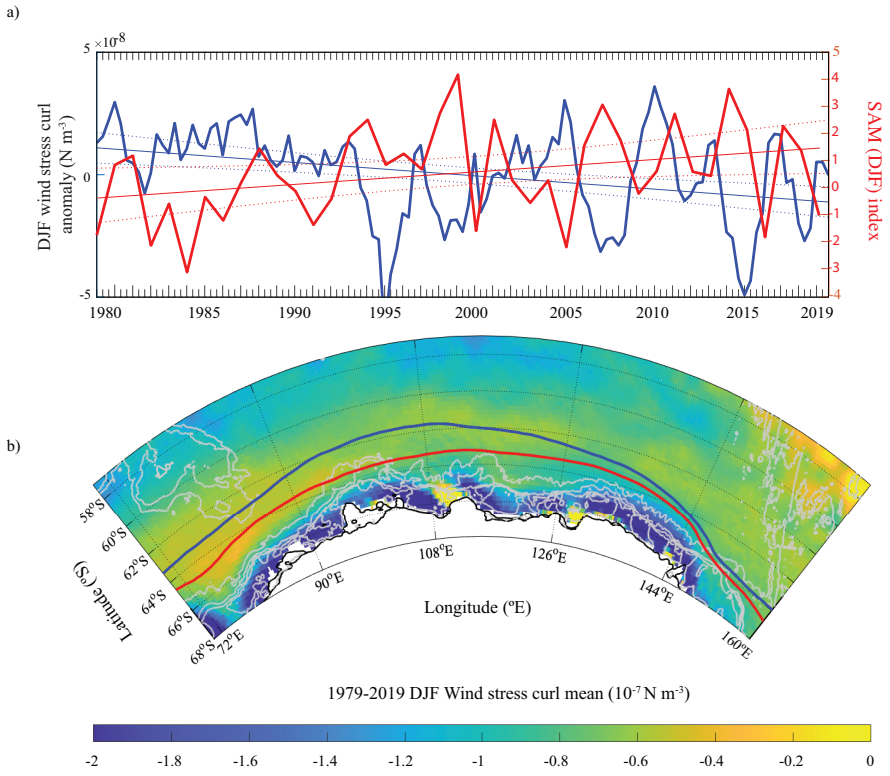

Figure 3. Changes in wind stress curl and their link to the southward migration of the S-ACC.

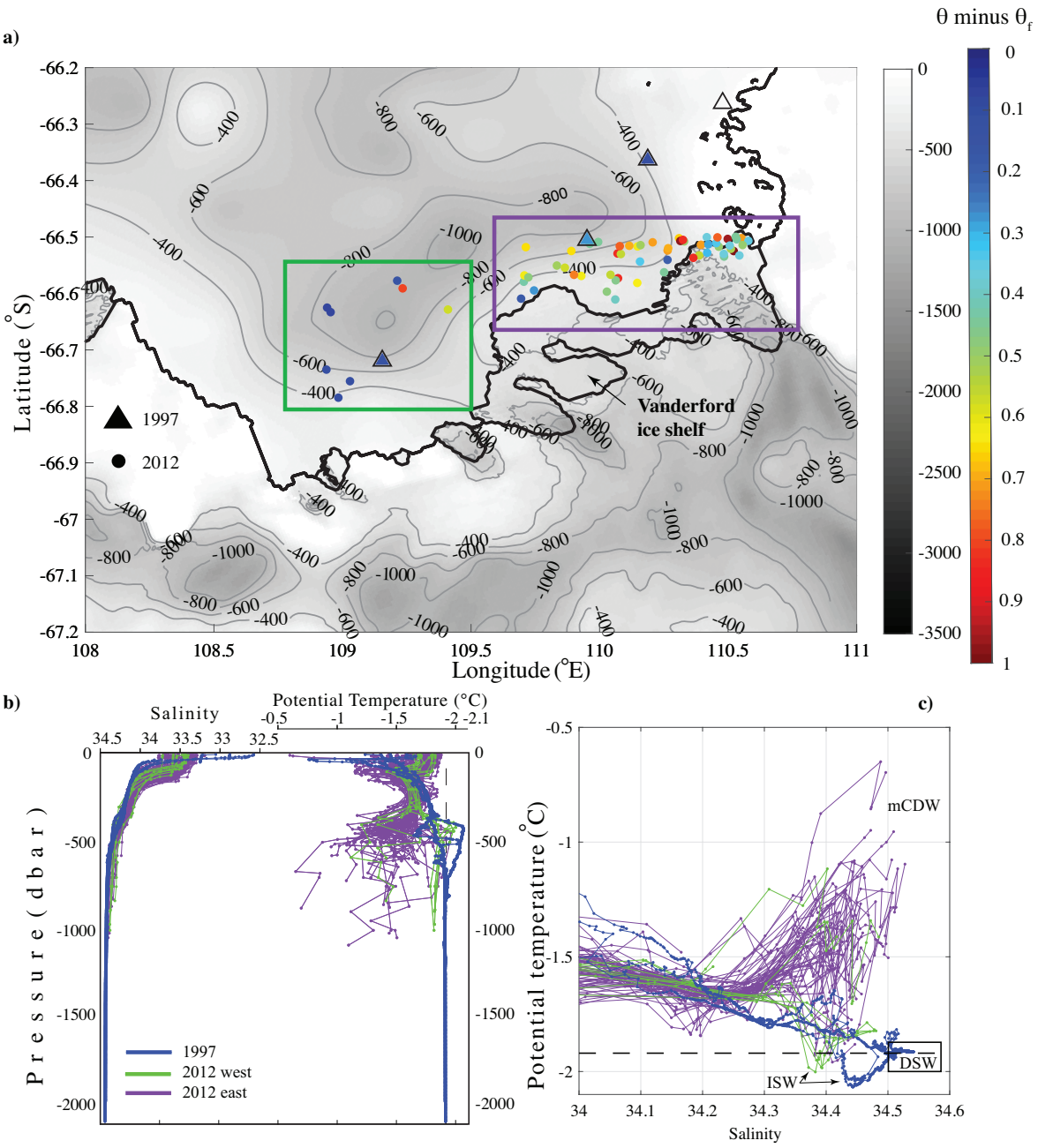

Figure 4. Warming of Vincennes Bay.

References

1. Rignot, E. et al. Four decades of Antarctic Ice Sheet mass balance from 1979–2017. *Proc. Nat. Acad. Sci.*, 116 (4), 1095–1103 (2019).
2. Jenkins, A. et al. West Antarctic Ice Sheet retreat in the Amundsen Sea driven by decadal oceanic variability. *Nature Geosci.*, 11 (10), 733–738 (2018).
3. Dotto, T. et al. Control of the oceanic heat content of the Getz-Dotson Trough, Antarctica, by the Amundsen Sea Low. *J. Geophys. Res. – Oceans*, 125 (8), e2020JC016113 (2020).
4. Fogt, R. and Marshall, G. J. The Southern Annular Mode: Variability, trends, and climate impacts across the Southern Hemisphere. *WIREs Climate Change*, 11 (4) (2020).
5. The IMBIE team., Shepherd, A., Ivins, E. et al. Mass balance of the Antarctic Ice Sheet from 1992 to 2017. *Nature,* 558, 219–222 (2018).
6. Rott, H., Rack, W., Skvarca, P. and Angelis, H. D. Northern Larsen Ice Shelf, Antarctica: further retreat after collapse. *Ann. Glaciol.*, 34, 277–282 (2002).
7. Schmidtko, S., Heywood, K. J., Thompson, A. F. and Aoki, S. Multidecadal warming of Antarctic waters. *Science,* 346, 1227–1231 (2014).
8. Holland, P. R., Bracegirdle, T. J., Dutrieux, P., Jenkins, A., and Steig, E. J. West Antarctic ice loss influenced by internal climate variability and anthropogenic forcing. *Nat. Geo.*, 12 (9), 718–724 (2019).
9. Smith et al. Pervasive ice sheet mass loss reflects competing ocean and atmosphere processes. *Science*, 30, eaaz5845 (2020).
10. Rintoul, S. R. et al. Ocean heat drives rapid basal melt of the Totten Ice Shelf. *Sci. Adv.,* 2, e1601610 (2016).
11. Herraiz–Borreguero, L. et al. Circulation of modified Circumpolar Deep Water and basal melt beneath the Amery Ice Shelf, East Antarctica. *J. Geophys. Res. Oceans*, 120, 3098–3112 (2015).

12. Greene, C. A., et al. Wind causes Totten Ice Shelf melt and acceleration. *Sci. Adv.*, 3, e1701681 (2017).
13. Gille, S. Warming of the Southern Ocean since the 1950s. *Science*, 295, 1275–1277 (2002).
14. Aoki, S., S. R. Rintoul, S. Ushio, S. Watanabe, and N. L. Bindoff. Freshening of the Adélie Land Bottom Water near 140°E. *Geophys. Res. Lett.*, 32, L23601, doi:10.1029/2005GL024246 (2005).
15. Yamakazi, K., et al. Multidecadal poleward shift of the southern boundary of the Antarctic Circumpolar Current off East Antarctica. *Science Advances*, 7 (24), 10.1126/sciadv.abf8755 (2021).
16. Auger, M., R. M., El. Kestenare, J-B Sallée and R. Cowley. Southern Ocean in-situ temperature trends over 25 years emerge from interannual variability. *Nature Communications*, 12, 514 (2021).
17. Velicogna, I., et al. Continuity of Ice Sheet Mass Loss in Greenland and Antarctica from the GRACE and GRACE Follow-On Missions, *Geo. Res. Lett*., 47 (8), e2020GL087291 (2020).
18. Konrad, H., A. Shepherd, L. Gilbert, A. E. Hogg, M McMillan, A. Muir and T. Slater. Net retreat of Antarctic glacier grounding lines, *Nat. Geo*.; https://doi.org/10.1038/s41561-018-0082-z (2018).
19. Nitsche, F. O., D. Porter, G. Williams, E. A. Cougnon, A. D. Fraser, R. Correia, and R. Guerrero. Bathymetric control of warm ocean water access along the East Antarctic Margin, *Geophys. Res. Lett.*, 44, 8936–8944, doi:10.1002/2017GL074433 (2017).
20. Paolo, F. S., Fricker, H. A., and Padman, L. Volume loss from Antarctic ice shelves is accelerating. *Science*, 348, 327-331, http://doi.org/10.1126/science.aaa0940 (2015).

21. Thompson, A. F., Stewart, A. L., Spence, P. and Heywood, K. J. The Antarctic Slope Current in a changing climate. *Rev. Geophys.*, 56, 741–770 (2018).

22. Whitworth, T. III, Orsi, A. H., Kim, S.–J., Nowlin Jr., W.D. and Locarnini, R. A., 1998. Water masses and mixing near the Antarctic Slope Front. Pp. 1–27 in Ocean, Ice and Atmosphere: Interactions at the Antarctic Continental Margin. Antarctic Research Series, vol. 75, S. S. Jacobs and R. F. Weiss, eds, American Geophysical Union, Washington, DC.

23. Meijers, A., Bindoff, N. L. and Rintoul, S. R. Estimating the four–dimensional structure of the Southern Ocean using satellite altimetry. *J. Atmos. Ocean. Tech.*, 28, 548–568 (2011).

24. Orsi, A. H., Whitworth, T., Nowlin, W. D. On the meridional extent and fronts of the Antarctic Circumpolar Current. *Deep Sea Res. I*, 42 (5), 641–673 (1995).

25. Swart, N.C., Fyfe, J.C., Gillett, N., and Marshall, G.J. Comparing trends in the southern Annular Mode and Surface Westerly Jet. *J. of Climate*, 28 (22), 8840-8859 (2015).

26. Naveira Garabato, A. C., et al. Phased response of the subpolar Southern Ocean to changes in circumpolar winds. *Geo. Res. Lett*., 46. https://doi.org/10.1029/2019GL082850 (2019).

27. Hazel, J. E. and Stewart, A. L. Are the Near–Antarctic Easterly Winds Weakening in Response to Enhancement of the Southern Annular Mode?. *J. Climate*, 32 (6) (2019).

28. Peña-Molino, B., M. S. McCartney, and S. R. Rintoul. Direct observations of the Antarctic Slope Current transport at 113E, *J. Geophys. Res.-Oceans*, 121, 7390–7407, doi:10.1002/ 2015JC011594 (2016).

29. Langlais, C., S. R. Rintoul, and J. D. Zika. Sensitivity of Antarctic Circumpolar Current Transport and eddy activity to wind patterns in the Southern Ocean. *Journal of Physical Oceanography*, 45 (4), 1051-1067 (2015).

30. Thompson, D. W. J., and S. Solomon. Interpretation of recent Southern Hemisphere climate change. *Science*, 296, 895–899 (2002).

31. Marshall, G. J. Trends in the Southern Annular Mode from Observations and Reanalyses, *J. Climate*, 16 (24), 4134–4143 (2003).

32. Spence, P., et al. Rapid subsurface warming and circulation changes of Antarctic coastal waters by poleward shifting winds. *Geophys. Res. Lett*., 41 (13), 4601–4610 (2014).

33. Ribeiro, N., Herraiz-Borreguero, L., Rintoul, S. R., McMahon, C. R., Hindell, M., Harcourt, R., and Williams, G. Warm modified Circumpolar Deep Water intrusions drive ice shelf melt and inhibit Dense Shelf Water formation in Vincennes Bay, East Antarctica. *J. Geophys. Res.-Oceans*, 126, e2020JC016998 (2021).

34. Tamura, T., Ohshima, K. I., Fraser, A. D., & Williams, G. D. Sea ice production variability in Antarctic coastal polynyas. *J. Geophys. Res.-Oceans*, 121(5), 2967–2979. https://doi.org/10.1002/2015jc011537 (2016).

35. Gordon, A. L. in Deep Convection and Water Mass Formation in the Ocean (eds Gascard, J. & Chu, P.) 17–35 (Elsevier, 1991).

36. Brancato, V. et al. Grounding line retreat of Denman Glacier, East Antarctica, measured with COSMO–SkyMed radar interferometry data. *Geophys. Res. Lett.*, 47, e2019GL08629 (2020).

37. Dutrieux, P., et al. Strong sensitivity of Pine Island Ice–Shelf melting to climatic variability. *Science*, 343, 174–178 (2014).

38. Zheng, F., Li, J., Clark, R. T., and Nnamchi, H. C. Simulation and projection of the Southern Hemisphere Annular Mode in CMIP5 models. *J. Clim.*, 26 (24), 9860–9879 (2013).

39. Silvano, A., et al. Freshening by glacial meltwater enhances melting of ice shelves and reduces formation of Antarctic Bottom Water. *Sci. Adv.*, 4 (4), eaap9467 (2018).

40. Khazendar, A., Schodlok, M.P., Fenty, I., Ligtenberg, S.R.M., Rignot, E., and van den Broeke, M.R. Observed thinning of Totten Glacier is linked to coastal polynya variability. *Nat. Comms.*, 4:2857, doi: 10.1038/ncomms3857 (2013).

Methods

Calculation of dynamic height from hydrographic profiles

We compute the dynamic height at 200 dbar relative to 1500 dbar for each hydrographic profile in our dataset north of the continental slope. By comparing profiles with the same dynamic height acquired at different times, we determine the temporal change in water mass properties (e.g., temperature) in a reference frame unaffected by frontal motions (Fig. S2). Our results are insensitive to the precise definition of dynamic height).

Decomposition of potential temperature changes

In order to assess the extent to which a CDW potential temperature change in geographical space ($\Delta\theta$) was associated with the long-term displacement of frontal features, we decomposed that change into components linked to ($\Delta\theta_{front}$), and disconnected from ($\Delta\theta'$), perturbations in dynamic height:

$$\Delta\theta(x,y,p) = \Delta\theta_{front}(x,y,z) + \Delta\theta'(x,y,z), \; z = -400 \; m.$$

$\Delta\theta(x,y,z)$ was quantified directly from the hydrographic observations by subtracting the potential temperature at 400 m prior to 1990 from the potential temperature at the same vertical level in 2010-2018 (Fig. 2a). These two periods were chosen to highlight the interdecadal change in CDW properties. To enable subtraction of potential temperatures from the two periods, hydrographic data were first grouped and averaged in bins of 0.5° of longitude by 0.5° of latitude, and, subsequently, differences were computed for each bin in which data were available in both periods (Fig. 2a).

The contribution of frontal displacements to changes in potential temperature was then calculated as

$$\Delta\theta_{front}(x,y,z) = \Delta\Phi(x,y) * d\theta/d\Phi(x,z), \; z = -400\ m.$$

Here, $\Delta\Phi(x,y)$ is the change in dynamic height between prior to 1990 and 2010-2018 (Fig. S2), and $d\theta/d\Phi(x,z)$ is the climatological change in potential temperature with respect to dynamic height (Fig. S9c). We defined $d\theta/d\Phi(x,z)$ by least-squares fitting a linear relationship to all potential temperature vs. dynamic height data available at 400 m (Fig. S9c). This fitting exercise was done in dynamic height bins of 0.05 $m^2\ s^{-2}$ between 0.35 and 0.75 $m^2\ s^{-2}$ (Fig. S9 b) and 10°-wide longitude bands between 80°E and 150°E (Fig. S9c), in order to account for gradual along-stream changes in hydrographic properties following the quasi-zonal circulation of the Southern Ocean. The percentage temperature change explained by frontal displacements was then estimated as $\Delta\theta_{front}(x,y,z)*100 / \Delta\theta(x,y,z)$ (Fig. 2b). Positive (negative) values mean that frontal displacements effect a same-signed (an oppositely-signed) potential temperature change to that observed at the depth used for the analysis (400 m).

The above method for assessing the influence of the S-ACC's southward migration on CDW warming cannot be applied in regions where the potential temperature at 400 m is below 1ºC and dynamic height ceases to decrease monotonically toward Antarctica (Fig. S9c). These regions encompass the continental slope and areas in which CDW shoals above 200 m (Fig. S9a, red circles).

Definition of the ACC's southern flank from hydrographic data and satellite altimetry

The ACC's southern flank (S-ACC) can be detected in a hydrographic section across the Southern Ocean as the zone where the 1.5°-1.8°C potential temperature class of CDW reaches its southern terminus and outcrops into the remnant winter mixed layer[24](Fig. S3) Commonly, this boundary zone is considered to include two distinct hydrographic fronts: the Southern ACC

Front and the Southern Boundary front proper[24]. However, in the eastern Indian Ocean sector of the Southern Ocean, these two fronts are often within tens of kilometres of each other[24] and translate meridionally in a coherent fashion, as seen in the repeat hydrographic sections in Figures S10 and S11. Thus, for the purposes of our work, we treat the S-ACC as a single, ~400-km wide feature. We opt for defining the S-ACC as the site at which the 1.8°C isotherm in CDW crosses a depth of 500 m, which approximately corresponds with the southern terminus of Upper CDW within the Indian sector or, equivalently, with the southernmost area in which CDW isopycnals outcrop steeply toward the surface (Figs. S10 and S11). While, using this definition, the S-ACC typically lies some 50-400 km to the north of the continental slope (depending on longitude), its meridional displacement affects waters as far south as the foot of the slope (e.g., Fig. S10a). Over the slope itself, the topographically-pinned Antarctic Slope Front separates ACC-sourced waters from cooler continental shelf waters [21,22]. Hence, encroachment of the S-ACC onto the slope is expected to press relatively warm varieties of CDW against the slope and increase the meridional temperature gradient there.

As the equivalent barotropicity of the ACC brings about a close correspondence between climatological water mass properties and dynamic height or sea surface height (Ψ_{SSH})[23], our hydrographic S-ACC definition can be re-cast in terms of Ψ_{SSH}, enabling tracking of the frontal zone's position from satellite altimetric observations. Inspection of repeat WOCE transects off East Antarctica, namely, WOCE I9 at ~110°E (occupied in 1995, 2005 and 2012) and WOCE SR3 at ~140°E (occupied in 1993, 1994, 2001, 2008 and 2011) reveals a very close match between our hydrographic definition of the S-ACC and the Ψ_{SSH} = -1.18 m contour in AVISO satellite altimetric data (Figs. S10 and S11). We thus adopt this Ψ_{SSH} value to determine the spatio-temporal evolution of the S-ACC over the period of altimetric measurements (1992-2018), and to examine the relationship between the frontal zone's proximity to East Antarctica

and the thickness change of the ice shelves in the region[20]. In order to avoid aliasing of the S-ACC's position by the seasonal (but irregular) sea ice cover, only altimetric data retrieved in the austral summer months (January to March) are considered in locating the front.

Data availability Statement

The data used in this study uses hydrographic measurements from the following public data centres: Southern Ocean database (http://woceatlas.tamu.edu), Argo float program (ftp://ftp.ifremer.fr/ifremer/argo), and the CCHDO data centre (http://cchdo.ucsd.edu). Also used are the Marine Mammal Exploring the Ocean Pole to Pole (MEOP) consortium data, which can be found at http://www.meop.net, and CTD and XCTD data from the Institute of Cetacean Research, found at https://www.icrwhale.org/oceanograhicdata.html. Bathymetric data were obtained from Rtopo 1.0.5 (https://doi.org/10.1594/PANGAEA.741917), and altimetric data via the AVISO (www.aviso.oceanobs.com/en/) and MyOcean (www.myocean.eu.org/) websites. The reanalysis wind data are available via the ECMWF website (www.ecmwf.int/). The 18-year Antarctic ice-shelf thickness time series was obtained from Dr. Fernando Paolo, and can be downloaded from https://sealevel.nasa.gov/data/dataset/?identifier=SLCP_ice_shelf_dh_v1_1. The Marshall Southern Annular Mode (SAM) index (station-based) is provided by Marshall, Gareth & National Center for Atmospheric Research Staff (Eds). "The Climate Data Guide: Marshall Southern Annular Mode (SAM) Index (Station-based)"; and can be retrieved from https://climatedataguide.ucar.edu/climate-data/marshall-southern-annular-mode-sam-index-station-based.

Code Availability Statement

Matlab scripts used for the analysis described in this study can be obtained from L H-B. on request.

Methods-only references

41. Herraiz-Borreguero, L. and A. C. Naveira Garabato, East_Antarctica, publisher (repository name), https://github.com/laurahebo-ocean/East_Antarctica.git, DOI: 10.5281/zenodo.6652320